doi:10.1038/nature11095

Supplementary Table 1. Summary of the binding between Angptls and various Ig-domain containing receptors as determined by flow cytometry analysis.

	Angptl1	Angptl2	Angptl3	Angptl4	GST-Angptl5	Angptl6	Angptl7
LILRA1	-	-	-	-	-	-	-
LILRA2	-	-	-	-	-	-	-
LILRA4	-	-	-	-	-	-	-
LILRB1	-	-	-	-	-	-	-
LILRB2	+	++	+/-	+/-	+++	+/-	+
LILRB3	-	+	-	-	+	-	-
LILRB4	-	-	-	-	-	-	-
LILRB5	-	+/-	-	-	+	-	-
Lair-1	+	+/-	+/-	-	+/-	+/-	+

The results were summarized from binding to LILRB2 transfected 293T cells and human cord blood LILRB2$^+$ cells. GST-Angptl1, 2, 3, 5, 6, 7 all bind to human cord blood LILRB2$^+$ cells.

Supplementary Table 2. Summary of the binding of differently tagged Angptl2 and Angptl5 to LILRB2.

Name	A2	A2-Flag	Flag-A2	A2-Flag	A2-CC-A5-FBN	A5-CC-A2-FBN	A5	GST-A5	GST-A5-Flag	A5-His
Manufacturer	In house (mammalian; could not be purified; in vivo CO-IP only)	In house (mammalian)	In house (bacterial)	In house (bacterial)	In house (mammalian)	In house (mammalian)	In house (mammalian; could not be purified; in vivo CO-IP only)	Abnova	In house (bacterial)	Gift from R&D Systems
Binding to LILRB2	++	++	+/-	+/-	++	++	++	+++	+++	+/-

A2 or A5: untagged Angptl2 or Angptl5

A2-Flag: Flag tagged at the C-terminus of Angptl2, mammalian-expressed (mammalian) or bacterially-expressed (bacterial)

Flag-A2: Flag tagged at the N-terminus of Angptl2

A2-CC-A5-FBN: the coiled-coil domain of Angptl2 fused to the fibrinogen-like domain of Angptl5

A5-CC-A2-FBN: the coiled-coil domain of Angptl5 fused to the fibrinogen-like domain of Angptl2

GST-A5-Flag: GST tagged at the N-terminus and Flag-tagged at the C-terminus of Angptl5

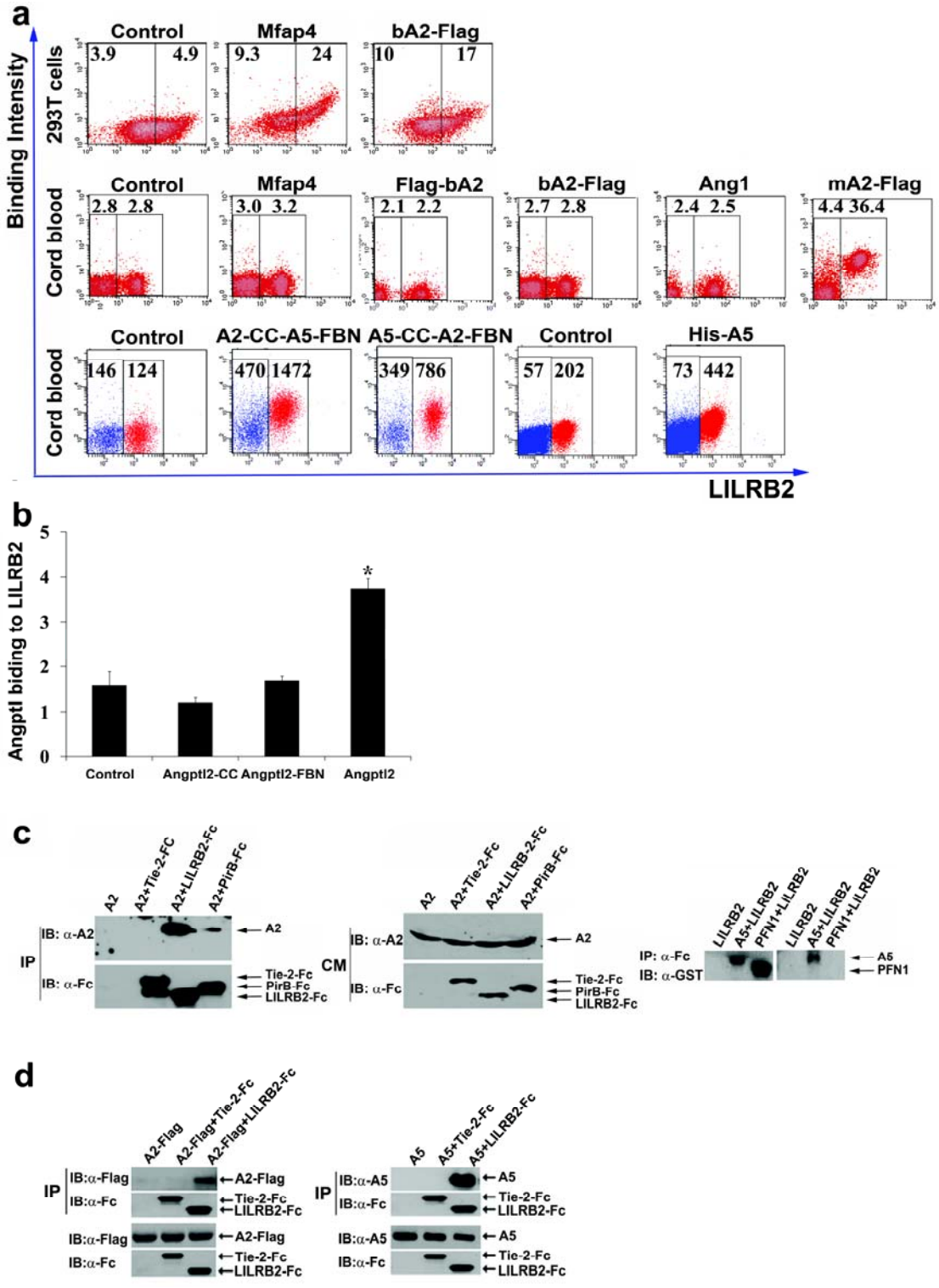
a
Binding Intensity
293T cells
Control
Mfap4
bA2-Flag
3.9
4.9
9.3
24
10
17
Cord blood
Control
Mfap4
Flag-bA2
bA2-Flag
Ang1
mA2-Flag
2.8 2.8
3.0 3.2
2.1 2.2
2.7 2.8
2.4 2.5
4.4 36.4
Cord blood
Control
A2-CC-A5-FBN
A5-CC-A2-FBN
Control
His-A5
146 124
470 1472
349 786
57 202
73 442
LILRB2
b
Angptl biding to LILRB2
Control
Angptl2-CC
Angptl2-FBN
Angptl2
c
A2
A2+Tie-2-FC
A2+LILRB2-Fc
A2+PirB-Fc
IP
IB: α-A2
IB: α-Fc
A2
Tie-2-Fc
PirB-Fc
LILRB2-Fc
CM
IP: α-Fc
IB: α-GST
LILRB2
A5+LILRB2
PFN1+LILRB2
A5
PFN1
d
A2-Flag
A2-Flag+Tie-2-Fc
A2-Flag+LILRB2-Fc
IP
IB:α-Flag
IB:α-Fc
A2-Flag
Tie-2-Fc
LILRB2-Fc
A5
A5+Tie-2-Fc
A5+LILRB2-Fc
IB:α-A5

Supplementary Figure 1. Angptl2 and Angptl5 bind LILRB2. a, Top, 293T cells transfected with CMV-LILRB2 were incubated with mammalian-expressed FLAG-tagged Mfap4 or bacterially-expressed Flag-tagged Angptl2, followed by staining with anti-FLAG-APC and anti-LILRB2-PE and flow cytometry analysis. Middle and bottom, human cord blood mononuclear cells were incubated with indicated FLAG-tagged Mfap4, bacterially-expressed FLAG-Angptl2, bacterially-expressed Angptl2-FLAG, mammalian-expressed Angiopoietin-1, mammalian-expressed FLAG-Angptl2, bacterially-expressed GST-A2-CC-A5-FBN-FLAG, GST-A5-CC-A2-FBN-FLAG, and His-tagged Angptl5, followed by staining with anti-FLAG-APC or anti-His-FITC and anti-human LILRB2-PE for flow cytometry analysis. **b,** Summary of the coiled-coil domain, fibronectin-like domain, and full-length Angptl2 binding to 293T cells transfected with LILRB2 as determined by flow cytometry. *, significantly different from control, $p < 0.05$ ($n = 3$, error bars, s.e.m). By contrast, the coiled-coil domain of Angptl2 bound to human cord blood LILRB2^{+} cells (not shown). **c,** Untagged Angptl2 bound to the extracellular domain of LILRB2 but not Tie-2 in conditioned medium (CM) of co-transfected 293T cells; GST-Angptl5 but not GST-Profilin-1 (as negative control) bound to the extracellular domain of LILRB2 *in vitro*. **d,** Purified Angptl2 or Angptl5 bound to the purified extracellular domain of LILRB2 but not that of Tie-2 *in vitro*.

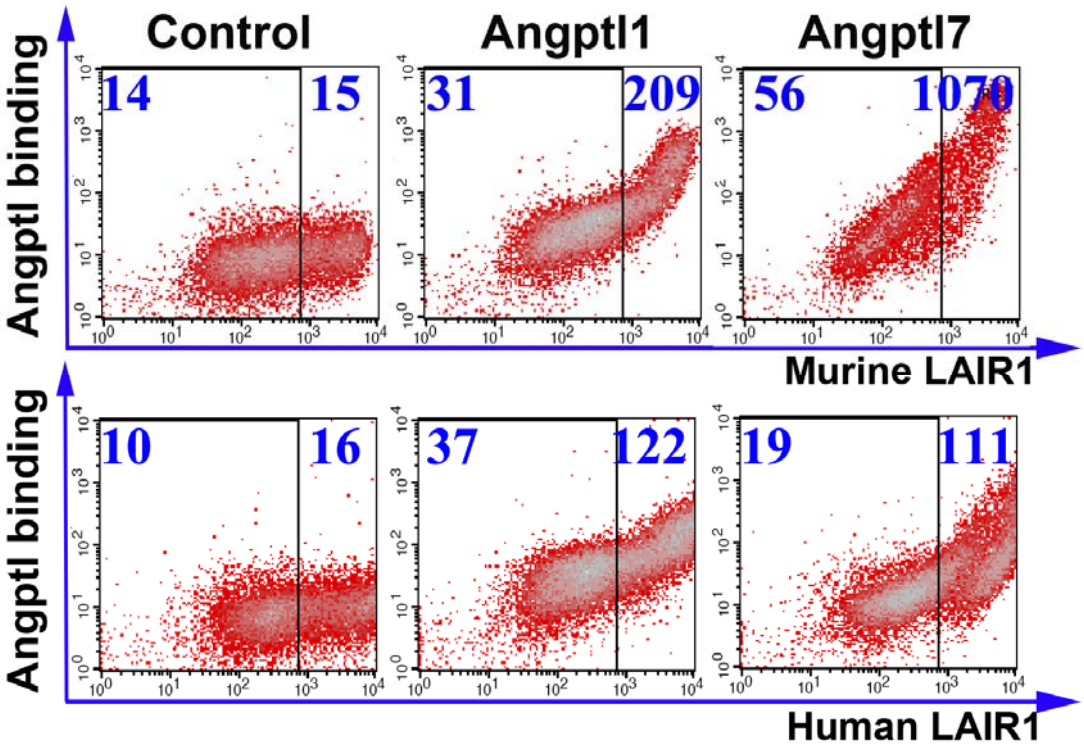

Supplementary Figure 2. Binding of Angptl1 and Angptl7 to 293T cells transfected with human and mouse LAIR1 as determined by flow cytometry. 293T cells transfected with CMV-mouse and human LAIR1 were incubated with indicated FLAG-tagged Angptls, followed by staining with anti-FLAG-APC and anti-LAIR1-PE in a flow cytometry analysis. Both mouse and human LAIR1 bind to Angptl1 and Angptl7 (upper panel and lower panel respectively).

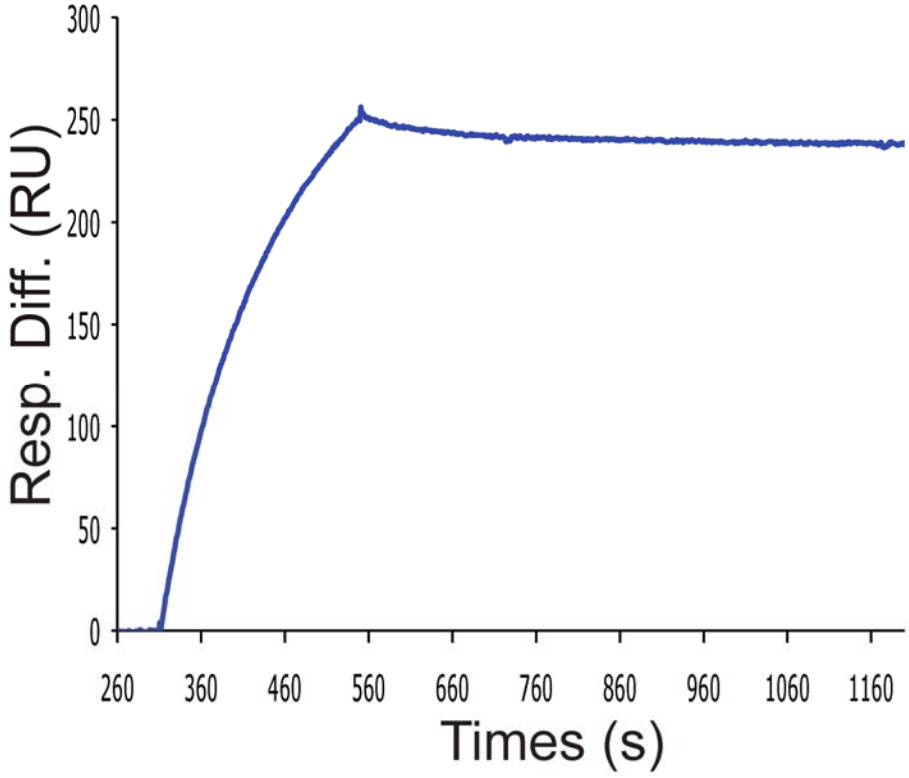

Supplementary Fig 3. Binding of GST-Angptl5 to LILRB2-hFc using SPR. The binding of purified Angptls to the LILRB2 extracellular domain fused to hFc was analyzed using a BIAcore 2000 and methods similar to those previously described [1]. Recombinant protein A (Pierce) was immobilized on two flow cells (~2,000 RU) of a CM5 sensor chip using the amine-coupling kit from GE. LILRB2-hFc was injected over one of the flow cells and captured by protein A to reach ~300 response units (RU). GST-Angptl5 (22.5 nM) was injected over the immobilized LILRB2 in HBS-EP (GE) containing 0.01 M HEPES (pH 7.4), 0.15 M NaCl, 0.005% polysorbate 20 at a flow rate of 30 μL/min. The sensorgram from the flow cell containing captured LILRB2-hFc was reference cell subtracted using the sensorgram from the protein A coupled flow cell. All measurements were performed at 25°C.

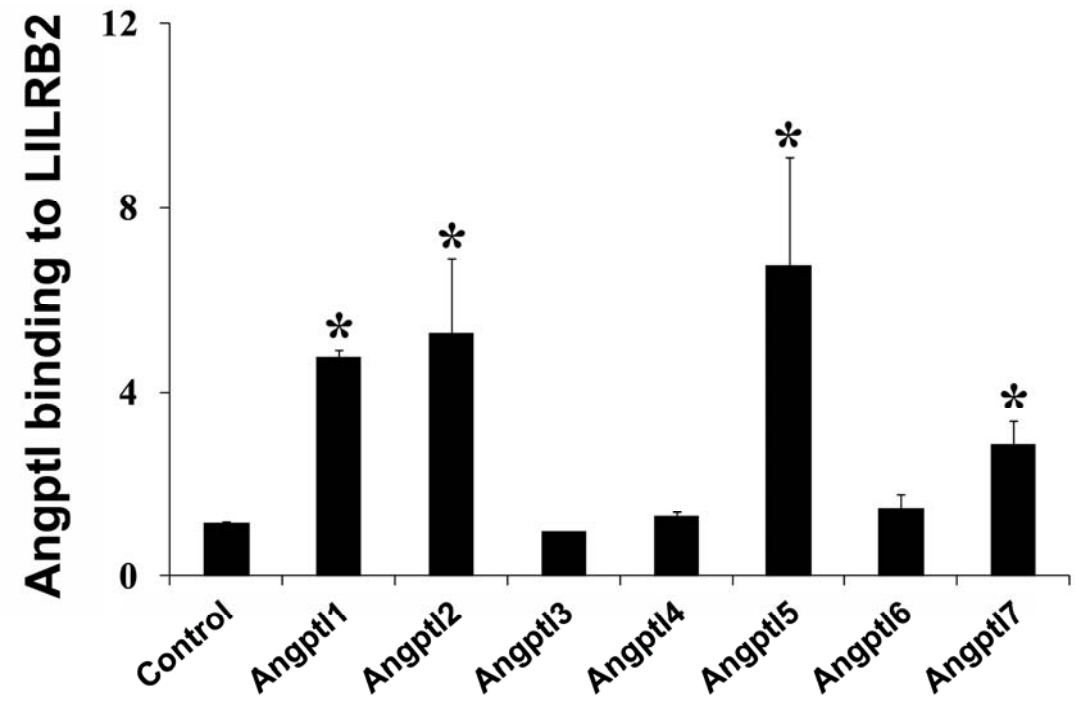

Supplementary Figure 4. Summary of Angptls binding to LILRB2$^+$ human cord blood cells as determined by flow cytometry. Relative binding was shown compared to control. *, significantly different from control, $p < 0.05$ ($n = 3$). Error bars, s.e.m.

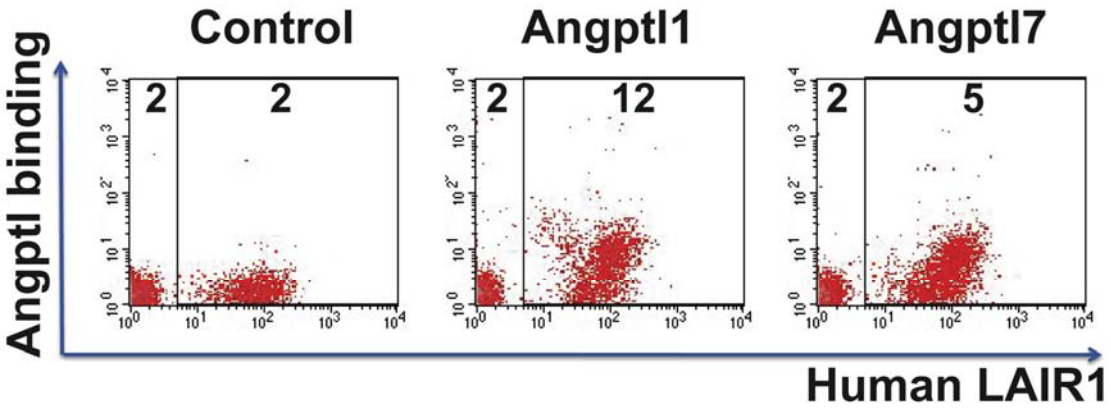

Supplementary Figure 5. Angptl1 and Angptl7 bind to LAIR1$^+$ human cord blood cells. Human cord blood mononuclear cells were incubated with indicated FLAG-tagged Angptl1 and Angptl7 followed by staining with anti-FLAG-APC and anti-human LAIR1-PE in a flow cytometry analysis.

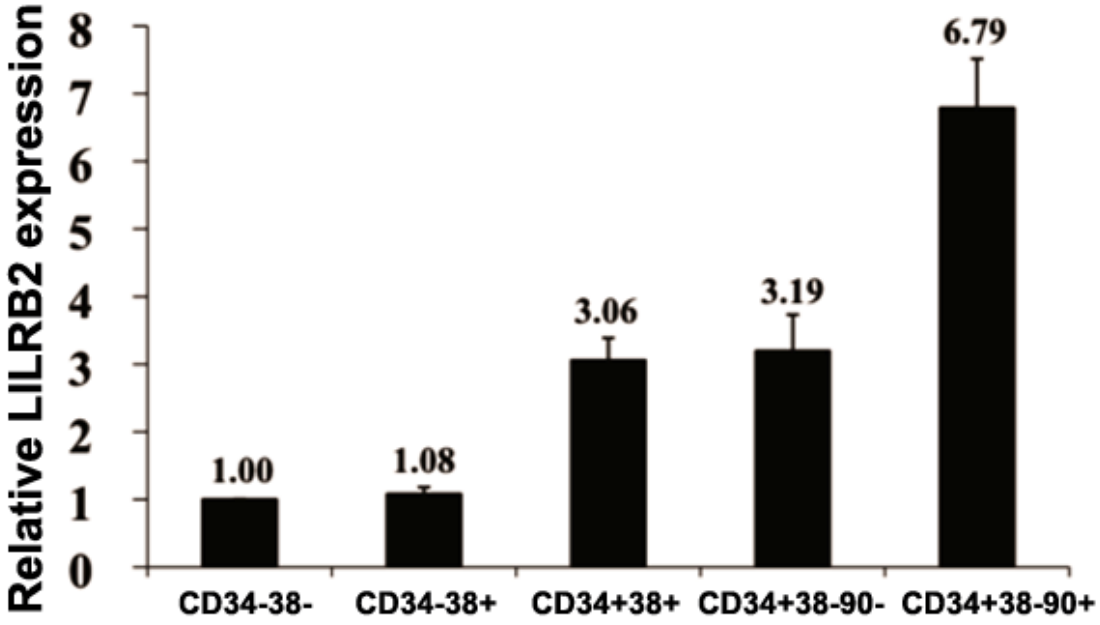

Supplementary Figure 6. Human cord blood $CD34^{+}CD38^{-}CD90^{+}$ cells express LILRB2 as determined by real-time RT-PCR (n = 3). Error bars, s.e.m.

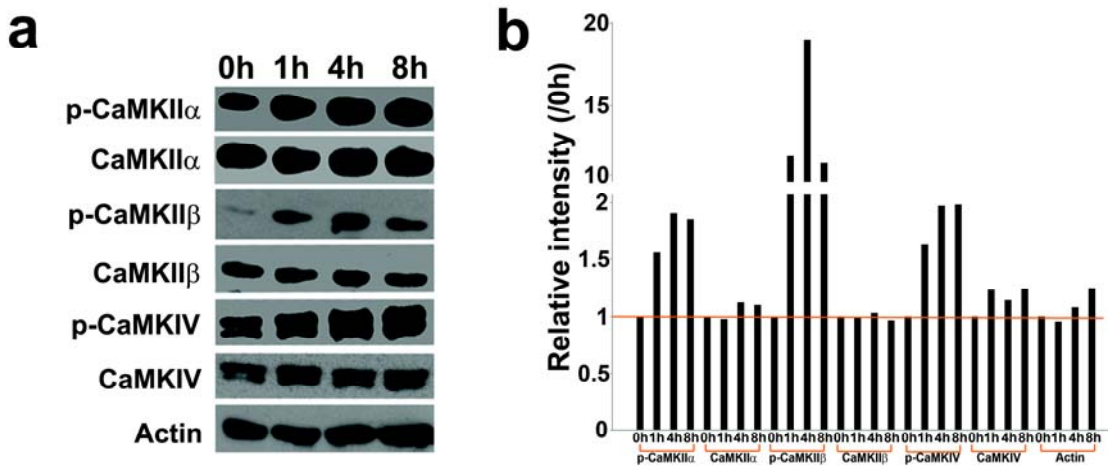

Supplementary Figure 7. GST-Angptl5 treatment increased the phosphorylation of human cord blood cells. a, Levels of phosphorylation and total amounts of CAMKII and CAMKIV in pre-starved human cord blood mononuclear cells incubated with 500 ng/ml GST-Angptl5 and 50 mM Na_3VO_4 for 0 to 8 h. **b,** Quantitation of band intensities of phosphorylated and total CAMKs in panel a.

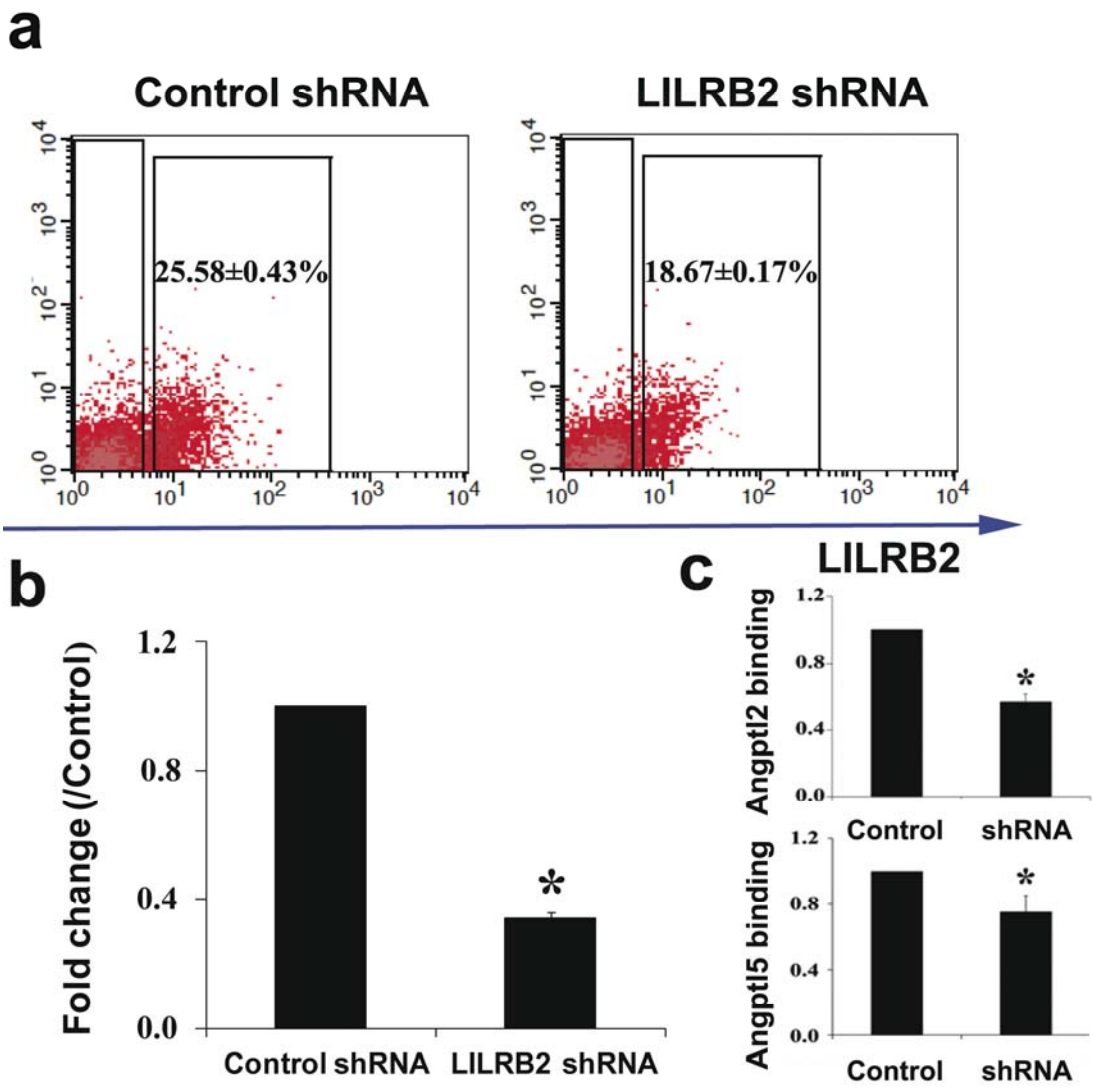

Supplementary Figure 8. Knockdown of LILRB2 by shRNA-encoding lentivirus in human cord blood mononuclear cells as determined by flow cytometry (a) and real-time RT-PCR (b) resulted in decreased binding to Angptl2 and GST-Angptl5 in human cord blood mononuclear cells (c). Scramble shRNA-encoding virus was used as control. * $p < 0.05$, $n = 5$. Error bars, s.e.m.

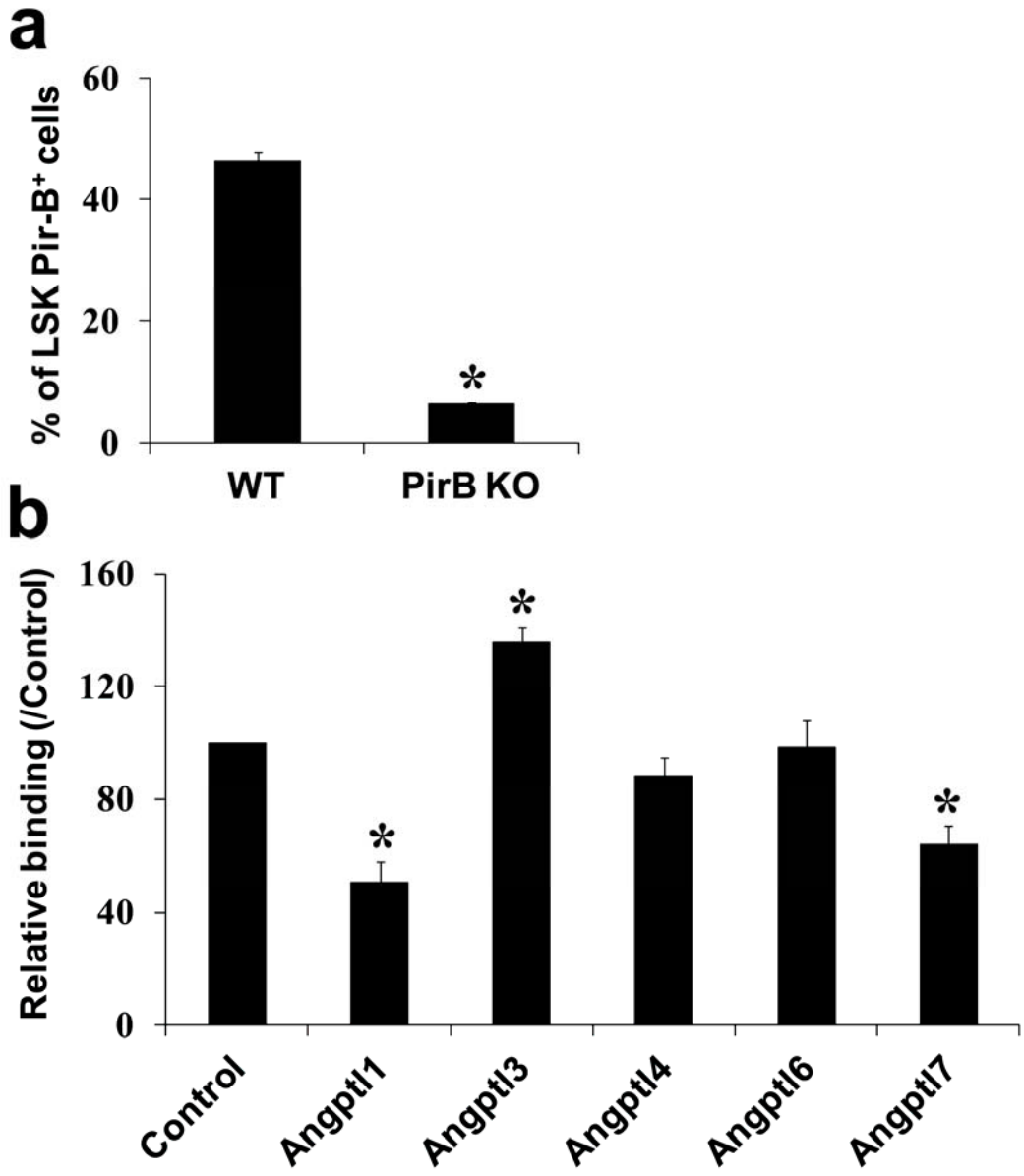

Supplementary Figure 9. Summary of Angptls binding to 293T cells transfected with PirB as determined by flow cytometry. a, PirB surface expression in WT but not in PirB knockout bone marrow cells as specifically determined by anti-PirB-PE (n = 3). The PirB knockout mice were described in [2]. **b,** Relative binding was shown compared to control. Angptl3 but not 1, 4, 6, 7 binds to PirB. *, significantly different from control, $p < 0.05$ (n = 3). Error bars, s.e.m.

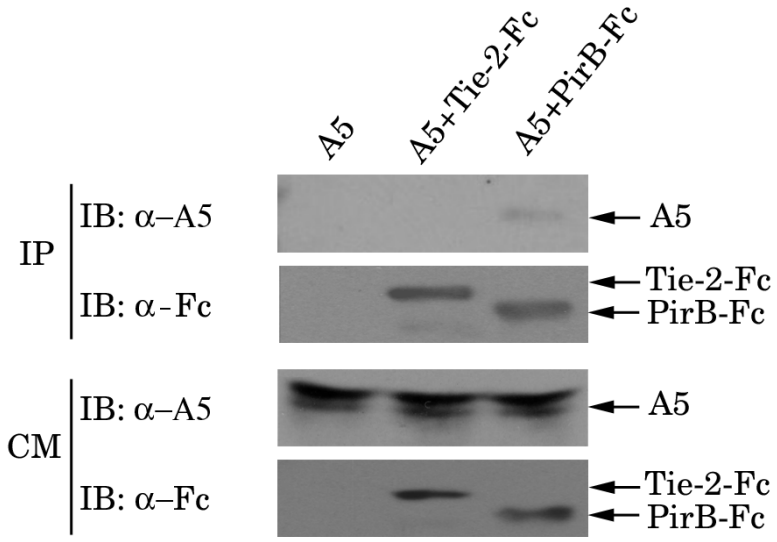

Supplementary Figure 10. Angptl5 bound to the extracellular domain of PirB but not the extracellular domain of Tie-2 in conditioned medium of co-transfected 293T cells.

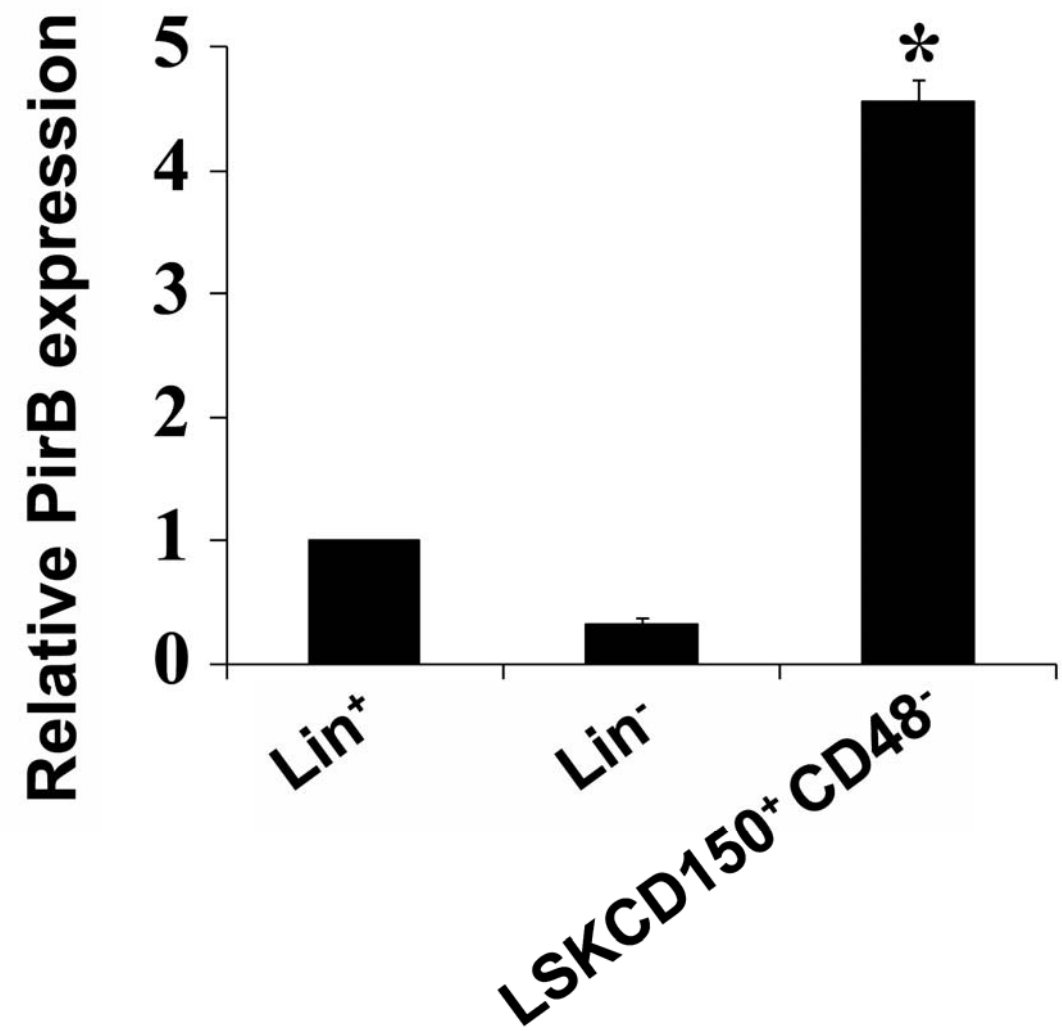

Supplementary Figure 11. Mouse BM HSCs express PirB as determined by real-time RT-PCR (n = 3). Error bars, s.e.m.

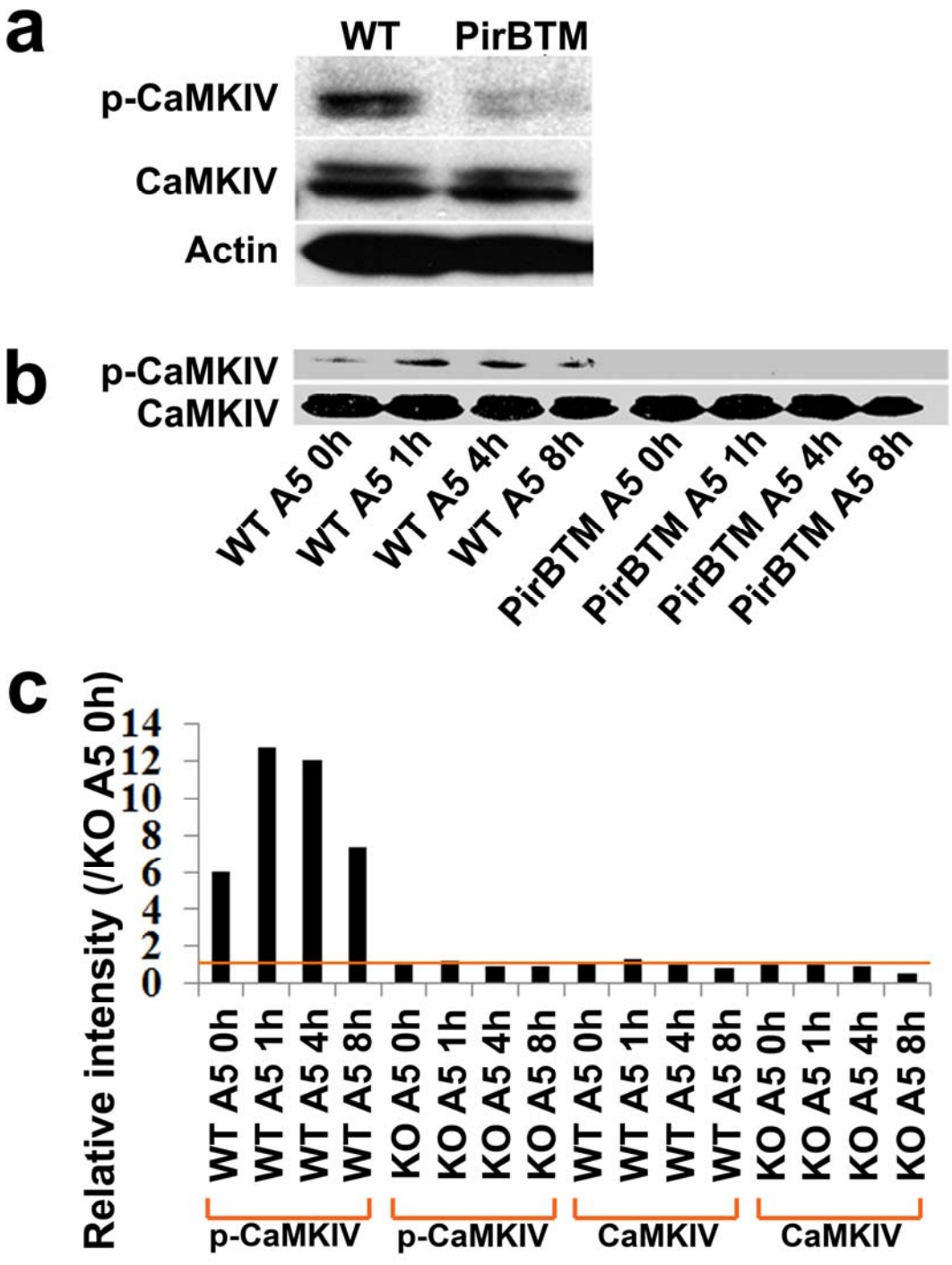

Supplementary Figure 12. PirB enhanced phosphorylation of CAMKIV in hematopoietic cells. a-b, Phosphorylation and amount of CAMKIV in freshly isolated

WT and PirBTM spleen cells (**a**) of 3 week old mice, and in pre-starved WT and PirBTM spleen cells incubated with 1 μg/ml GST-Angptl5 and 50 mM Na_3VO_4 for 0 to 8 h (**b**). (**c**) Quantitation of band intensities of phosphorylated and total CAMKIV in panel **b.**

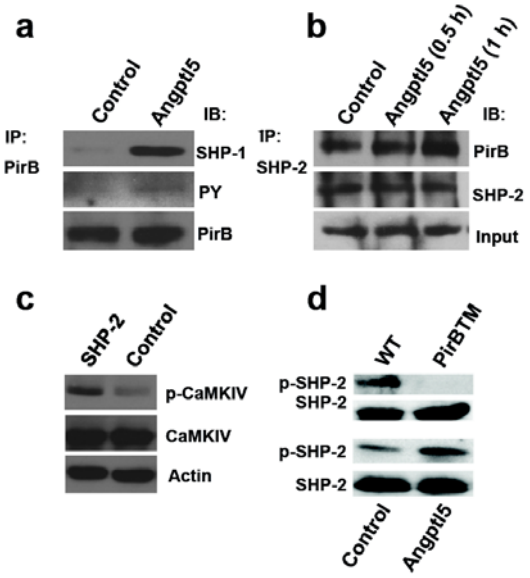

Supplementary Figure 13. Angptl5 binding increases phosphorylation of PirB and association between PirB and SHP-1/SHP-2. a, Angptl5 treatment of mouse splenocytes led to increased association between PirB and SHP-1 (top blot) and enhanced phosphorylation of PirB (as detected by anti-pTyr 4G10 in the middle blot). 5-7 x 10^7 WT spleen cells isolated from 4-6-week old mice were pre-starved in 5 ml serum-free medium for 5 h at 37 °C and incubated with 300-500 ng/ml GST-Angptl5 and 20 mM Na_3VO_4 for 1 h. The cell lysytes were immunoprecipitated by anti-PirB and probed by anti-SHP-1, anti-pTyr, and anti-PirB respectively. **b,** 1 h of Angptl5 treatment of mouse splenocytes led to increased association between PirB and SHP-2. Cells were treated as in panel A followed by immunoprecipitated by anti-SHP-2 and probed by anti-PirB and anti-SHP-2 respectively. **c,** Spleen cells isolated from AML mice transplanted with SHP-2 overexpressed PirBTM MLL-AF9 AML cells showed induced phosphorylation of CAMKIV. **d,** Phosphorylation and amount of SHP-2 in freshly isolated WT and PirBTM AML cells (top) and pre-starved WT AML cells incubated with 500 ng/ml GST-Angptl5 and 20 mM Na_3VO_4 for 1 h (bottom).

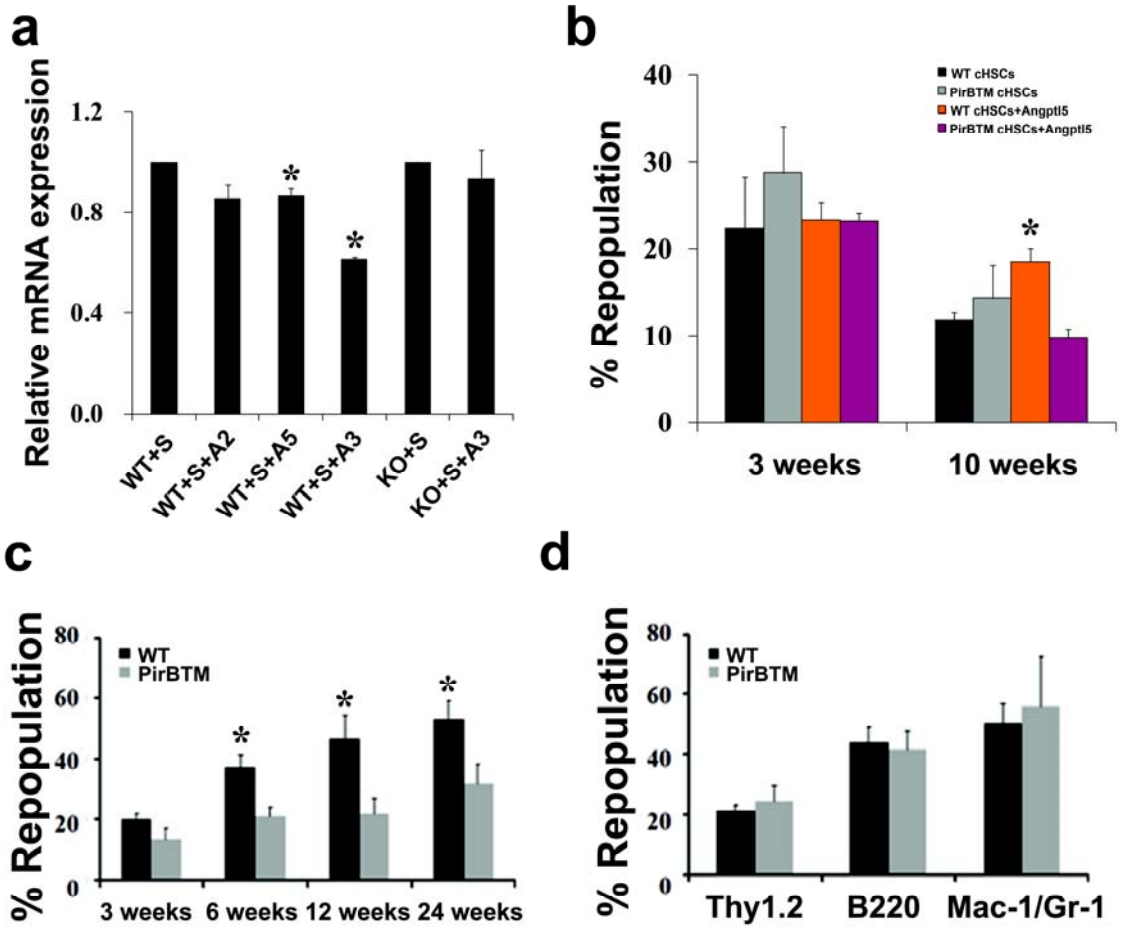

Supplementary Figure 14. Angptls inhibit Ikaros expression in WT but not in PirBTM HSCs and support HSC repopulation through PirB. a, The real-time RT-PCR analysis of WT or PirBTM bone marrow $Lin^{-}Sca\text{-}1^{+}Ki^{t+}Flk2^{-}CD34^{-}$ cells cultured in SCF-containing serum-free medium, treated with or without 500 ng/mL Angptl2, Angptl3, or Angptl5 for 24 hours. Gene expression in untreated samples was normalized to 1 (n = 6). **b**, GST-Angptl5 enhances *ex vivo* expansion of mouse adult BM HSCs through PirB. Eight-day cultured progenies of input equivalent 150 $Lin^{-}Sca\text{-}1^{+}Kit^{+}CD34^{-}Flk2^{-}$ BM HSCs from CD45.2 C57BL/6 WT or PirBTM donors were co-transplanted with 100,000 freshly isolated CD45.1 BM competitors into lethally irradiated CD45.1 recipients (n = 5, *, $p < 0.05$, significantly different from the value of PirBTM HSCs

treated by Angptl5). **c,** Competitive reconstitution of $1x10^5$ fetal liver cells from WT or PirBTM donors. Left, donor repopulation at 3-24 weeks post-transplantation (n = 5). **d,** multilineage contribution at 24 weeks post-transplantation (n = 5). Here "% Repopulation" refers lineage composition in the CD45.2 donor population. Error bars, s.e.m.

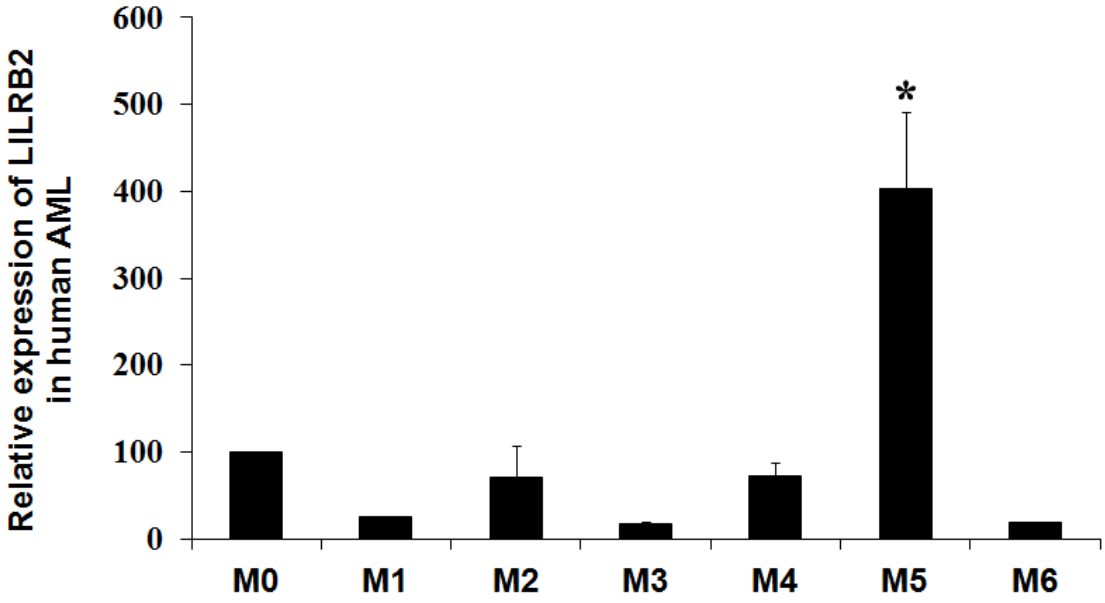

Supplementary Figure 15. The LILRB2 expression is significantly higher in blood of M5 AML patients. LILRB2 mRNA expression data were obtained by extracting LILRB2 gene from a pool of 9004 samples as described in [3]. *, Significantly different compared to the pool of 9004 samples, $p < 10^{-7}$. Error bars, s.e.m.

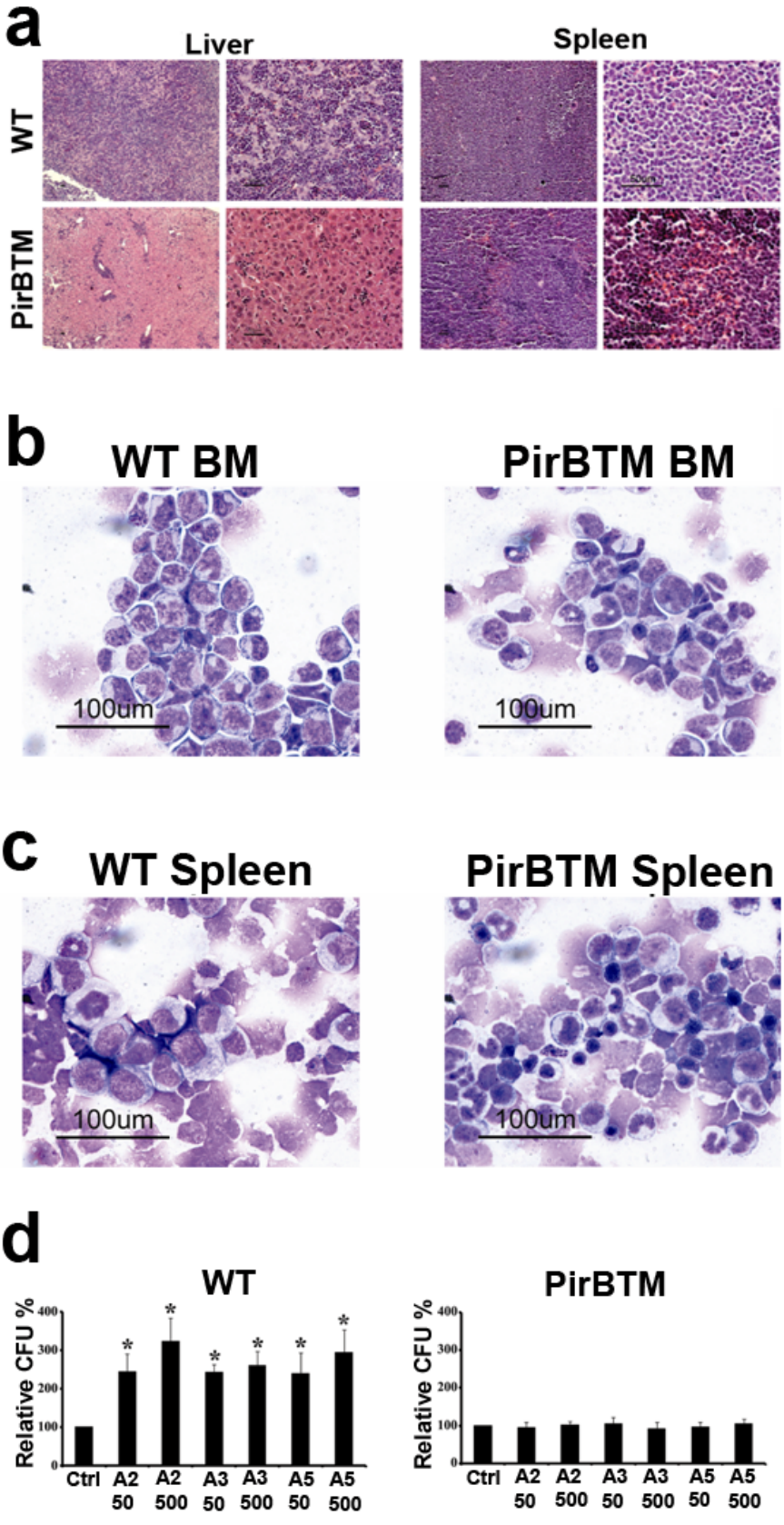
a
Liver
Spleen
WT
PirBTM
b
WT BM
PirBTM BM
100um
100um
c
WT Spleen
PirBTM Spleen
100um
100um
d
WT
PirBTM
Relative CFU %
400
300
200
100
0
Ctrl
A2 50
A2 500
A3 50
A3 500
A5 50
A5 500

Supplementary Figure 16. PirB supports MLL-AF9 AML development. a, Histological analysis of AML infiltration in the livers and spleens of WT and PirBTM AML transplanted mice at 28 d (hematoxylin/eosin staining). **b-c,** Cytospin preparations of bone marrow (b) and spleen (c) from MLL-AF9 WT and PirBTM mice. **d,** CFUs formed from WT or PirBTM $YFP^{+}Mac\text{-}1^{+}Kit^{+}$ AML cells with indicated ng/ml of Angptls (n = 3). * $p < 0.05$. Error bars, s.e.m.

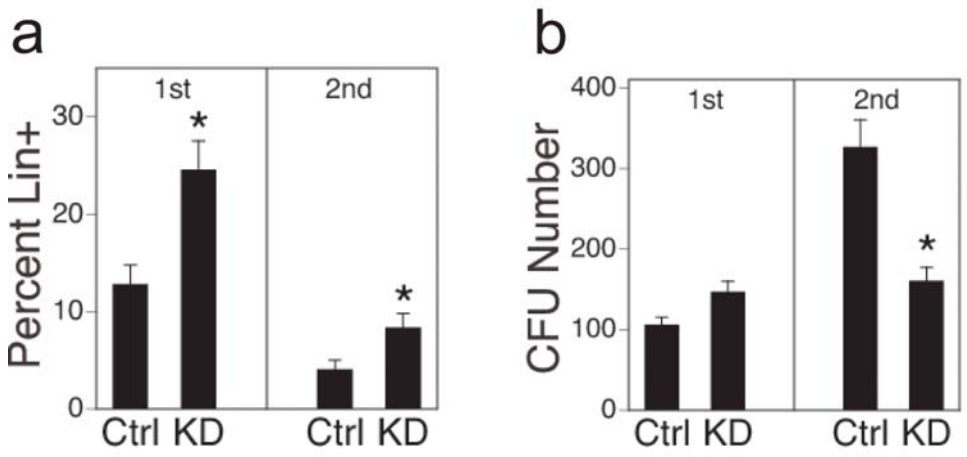

Supplementary Figure 17: Knockdown of Angptls increased differentiation and decreased replating efficiency of human cord blood HSCs. a-b, Knockdown of Angptl1-7 on human cord blood CD133$^+$ cells by shRNA lentiviruses increased Lin$^+$% (**a**) and decreased replating efficiency (**b**). Human cord blood CD133$^+$ cells were cultured for primary and secondary CFU assays for 12 days before they were collected for analyses. Results are shown as the mean ± SD for an experiment in which 500 CD133$^+$ cells were plated per ml in primary CFU assay and ¼ from which for subsequent 2nd replating (n = 3; $p < 0.05$). Error bars, s.e.m.

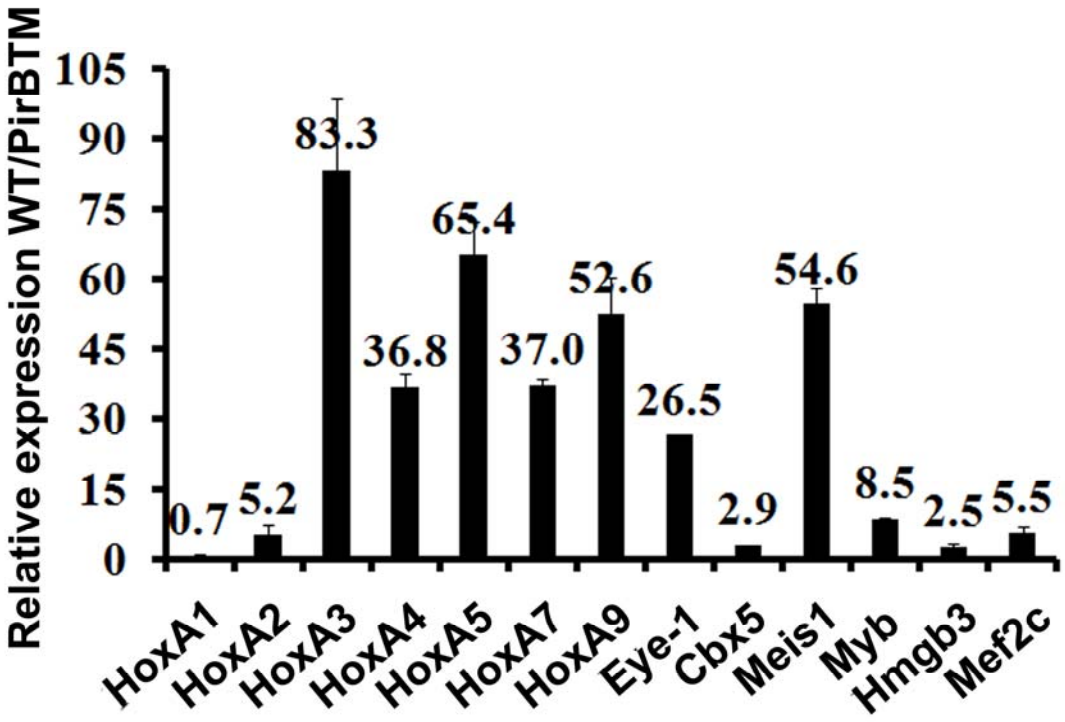

Supplementary Figure 18. PirBTM Mac-1^{+}Kit^{+} cells have decreased levels of mRNAs of certain AML-related oncogenes compared to WT counterparts as determined by real-time RT-PCR (n = 3). Error bars, s.e.m.

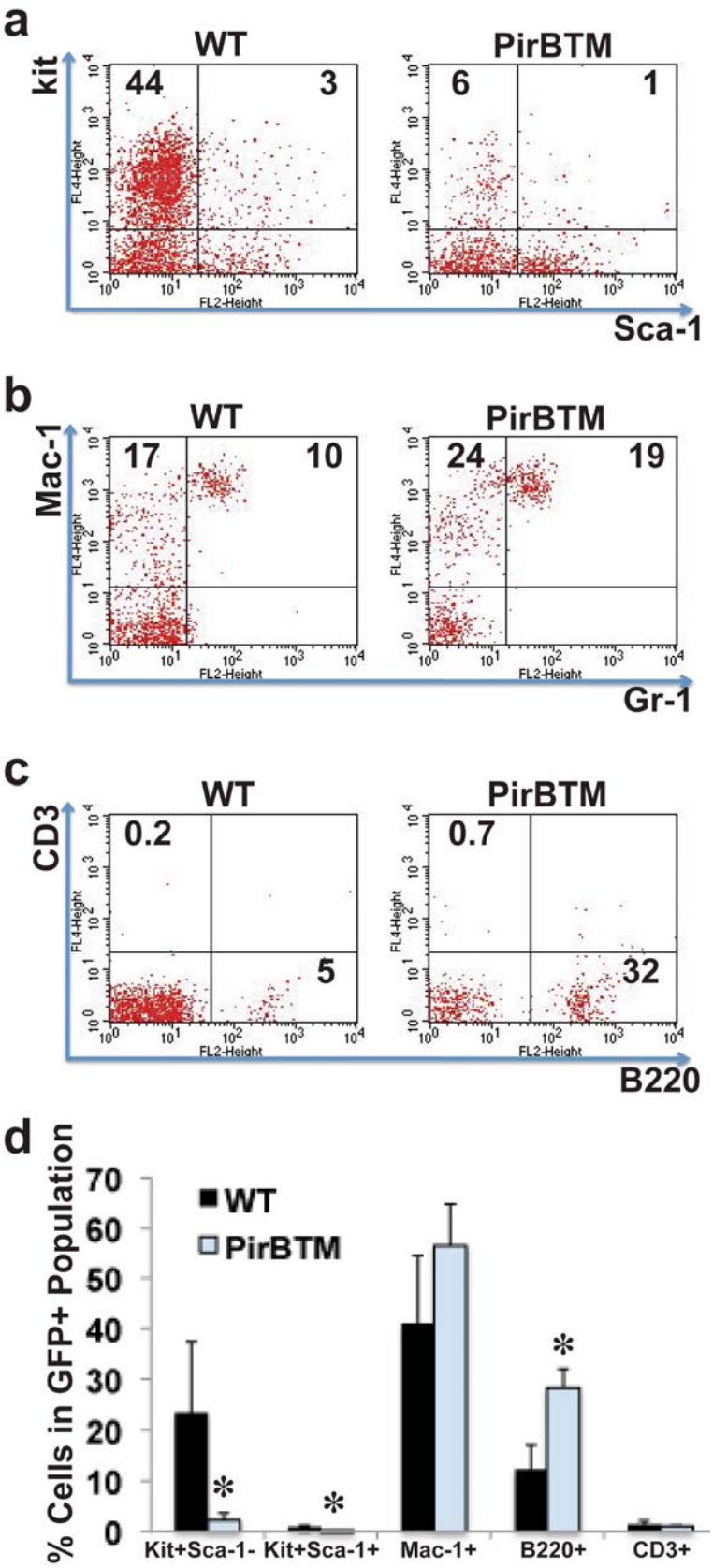
a
WT
PirBTM
kit
44
3
6
1
Sca-1
b
WT
PirBTM
Mac-1
17
10
24
19
Gr-1
c
WT
PirBTM
CD3
0.2
5
0.7
32
B220
FL4-Height
FL2-Height
d
% Cells in GFP+ Population
WT
PirBTM
70
60
50
40
30
20
10
0
Kit+Sca-1-
Kit+Sca-1+
Mac-1+
B220+
CD3+

Supplementary Figure 19. PirB suppresses differentiation and increases frequency of the progenitors of AML1-ETO9a (AE9a) induced leukemia. a-c, Representative flow cytometry plots showing that PirBTM AE9a AML mice (as described [4]) have decreased $Kit^+Sca\text{-}1^-$ and $Kit^+Sca\text{-}1^+$ progenitors but increased differentiated cells relative to mice transplanted with WT cells in the peripheral blood at 2.5 months after transplantation. **d**, Summary of the percentages of lineage marker expression in the GFP^+ ($AE9a^+$) peripheral blood of mice at 2.5 months after transplantation (n = 8; * significantly different from wild-type values, $p < 0.05$). Error bars, s.e.m.